J Mol Model (2013) 19:3255–3261
DOI 10.1007/s00894-013-1860-6

ORIGINAL PAPER

Structures and stabilities of ScB_n (n=1–12) clusters: an *ab initio* investigation

Jianfeng Jia · Lijuan Ma · Jian-Feng Wang · Hai-Shun Wu

Received: 5 January 2013 / Accepted: 17 April 2013 / Published online: 7 May 2013

Abstract The geometries, stabilities, and electronic properties of ScB_n (n=1–12) clusters have been systematically investigated by using density functional theory B3LYP method and coupled–cluster theory CCSD(T) method. It is found that the ground state isomers of ScB_n have planar or quasi–planar structure when $n \leq 6$, which can be viewed as a B atom of the corresponding B_{n+1} cluster is substituted by a Sc atom. From $n \geq 7$, the ground state isomers favor nest–like structure, in which the Sc atom sits on a nest–like B_n cluster. The calculated second–order differences of energies manifest that the magic numbers of stability are n=3, 7, 8, 9 and 11 for the ScB_n clusters. Further analysis indicates that the ScB_7 cluster with C_{6v} symmetry represents the outstanding stable ScB_n cluster, as confirmed by its electronic structure and molecular orbitals.

Keywords *Ab initio* calculation · Electronic structure · ScB_n cluster · Stability

Introduction

As promising candidate materials for hydrogen storage, the transition metal (TM) doped B_n nanostructures have attracted broad attentions and prompted further investigations. Meng [1] pointed out that the boron nanotubes decorated by Ti atoms can achieve 5.5 wt% hydrogen storage capacity. Zhao and his coworkers [2] designed a new type of hydrogen storage media, chained TiB_x, and they found that the most stable TiB_5 chain can achieve 7.3 wt% hydrogen storage capacity with the average binding energy per hydrogen molecule 43.7 kJ mol^{-1}. Moreover, icosahedral B_{60}, B_{80} decorated by scandium atoms also were reported as promising hydrogen materials predicted by theoretical calculations [3–6]. It was predicted that $Na_{12}B_{80}$ has the greatest hydrogen capacity of 11.2 %, however with small adsorption energy of about 0.07 eV per hydrogen molecule [7]. $Sc_{12}B_{80}$ was reported a hydrogen capacity of 7.9 wt% with the proper adsorption energy of 0.34 eV [5]. Recently, Zhao [8] found that the most stable B_{80} and other medium–sized boron clusters have core–shell structures rather than hollow cages. Quarles [9] reported that the most stable boron fullerene consists of 12 filled pentagons and 12 additional hollow hexagons, which is more stable than the empty pentagon boron fullerenes. These results indicated that more attempts are needed to understand the structure of TM doped boron clusters fundamentally. It is both necessary and interesting to further investigate the TM doped boron clusters so as to provide detailed information about the influence of TM doping on the host B_n clusters. On the other side, there is increasing attention on the growth pattern and electronic properties of metallic atom doped boron clusters due to the practical values of metal–boron systems in many fields. For example, Zhai and coworkers [10] reported the electronic and chemical bonding properties of B_7Au_2 and $B_7Au_2^-$ with photoelectron spectroscopy. Spectroscopic parameters of LiB_n (n=6, 8) were determined by Alexandrova *et al.* [11, 12]. There are also lots of theoretical works reported on the structures and stabilities of small metallic atom doped boron clusters [13–19].

To understand the growth pattern and the nature of chemical bonding in larger clusters, it is necessary to have a good understanding of small clusters. In this work, we perform an extensive search for the lowest–energy structures of the ScB_n (n=1–12) clusters. The main purpose is to offer theoretical understanding and interpretation of the relative stability, growth behavior and electronic structure of ScB_n, at the same time, to examine the effects of the doped Sc atom on the pure boron clusters.

J. Jia (✉) · L. Ma · J.-F. Wang · H.-S. Wu
School of Chemical and Material Science,
Shanxi Normal University, Linfen 041004, China
e-mail: jiajf@dns.sxnu.edu.cn

Computational details

The geometry of the ScB_n (n=1–12) isomers were optimized at the level of density functional theory (DFT) with Becke's [20] three–parameter exchange and Lee–Yang–Parr correlation functional [21] implemented in Gaussian 03 program [22]. The split valence basis set with diffusion functional, namely 6–311+G(d) was employed to describe the orbital of all atoms involved. Geometry optimizations were done with no symmetry restriction. For ScB_n with even n, the multiplicities of 2, 4 and 6 were considered, while for odd n, multiplicities of 1, 3 and 5 were considered. All the reported isomers were characterized as energy minima by frequency calculations at the same level. The zero–point energies also were obtained at this theoretical level. Feng [19] demonstrated that B3LYP/6-311+G(d) method can repeat the experimental values of bond length, vibration frequency and binding energy of the B_2 dimer well.

In order to get the lowest–energy structures of ScB_n clusters, other than optimization of independent configurations, we have also optimized some structures by substituting one B atom of stable B_{n+1} cluster by Sc atom, or by placing one Sc atom on each possible site of the stable B_n clusters, as well as by adding one B atom to the stable ScB_{n-1} clusters.

As regards the relative stability of TiB_n and B_n, our recently study [23] showed that DFT method occasionally gives different result from the more accurate CCSD(T) method. It was found that the CCSD(T) method, equipped with cc–pvtz basis set can reproduce the triple ground–state of B_2 dimer determined by experiment [23]. So, the single point calculations at CCSD(T)/cc–pvtz level on the geometries optimized at B3LYP/6–311+G(d) were carried out for stable ScB_n isomers to get more reliable energies. The relative energies for ScB_n at B3LYP level differ from those at CCSD(T) level, but they show the same order and trend in a qualitative way. Thus, only the CCSD(T) single energetics with ZPE corrections (obtaining at B3LYP/6–311+G(d) level) were used for discussions and comparisons.

Results and discussion

Equilibrium geometries

By employing the described computational scheme described in computational details, we have explored a number of low–lying isomers and determined the lowest–energy structures for the ScB_n clusters up to n=12. The predicted ground state (G–S) structures and some low–lying metastable isomers were shown in Figs. 1 and 2. The G–S structures of pure B_n clusters [24] were also plotted in Figs. 1 and 2 for comparisons.

The ground state of ScB is a quintet isomer, which is more stable than the triplet and the singlet by 0.05 and 0.50 eV, respectively. Most of MB dimers (M = Ti, Cr,

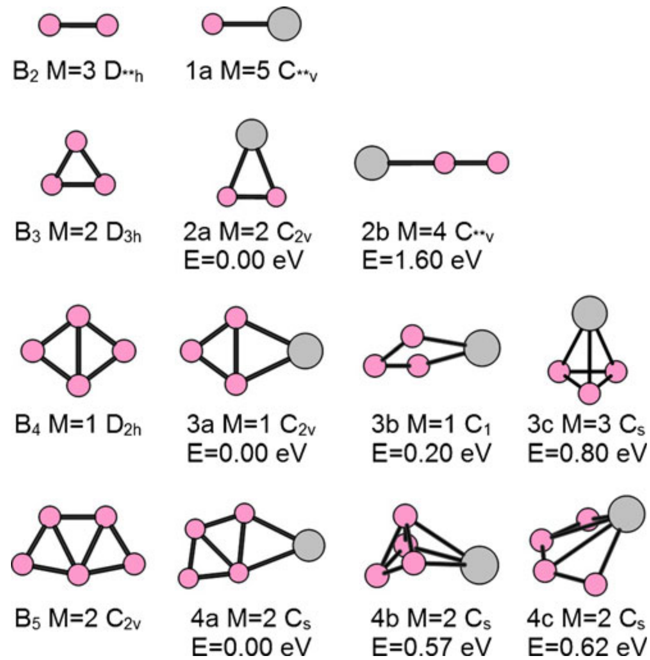

Fig. 1 Equilibrium geometries, the symmetries and spin multiplicities of the B_n (n=2–5) and ScB_n (n=1–4) structures. Relative energies (E) are given in eV

Mn, Fe, Co) have high spin multiplicity (6, 6, 5, 4, 3, respectively) [15], which is related to the un–bonded d orbitals of transition metal atom. The bond length of Sc–B (2. 088 Å) is longer than that of reported Ti–B (2.06 Å) [23], Fe–B (1. 74 Å) and Ni–B (1.71 Å) [15].

All the G–S structures of ScB_n clusters with $n≥2$ are singlet state (when n is odd number) or doublet state (when n is even number). The G–S structure of ScB_2, as shown in Fig. 1 as 2a, has isosceles triangular shape (C_{2v}), with two Sc–B bonds of 2.12 Å, and one B–B bond of 1.54 Å. In fact, most MB_2 isomers have triangular shape, including M = Li, Al, Ti, Cr, Mo, Fe, Co, Ni [15–17, 19]. The quartet linear chain 2b isomer, in which Sc bonds to one B atom, is higher in energy than the G–S structure 2a by 1.60 eV. Another linear form in which Sc atom is located at the center of two B atoms turns out to be very unstable. The stabilities of these three ScB_2 indicate that B atom trends to bond with B atom.

For ScB_3, the planar rhombus isomer 3a in Fig. 1 is the lowest–energy isomer, which can be viewed as a B atom of most stable B_4 [24] being substituted by a Sc atom. The non–planar rhombic isomer 3b is slightly higher in energy than 3a by 0.20 eV. The pyramid structure 3c is substantially higher in energy than the lowest–energy structure by 1.03 eV. It is interesting to notice that all MB_3 (M = Sc, Ti, Cr, Mn, Fe, Co, Ni) [15, 23] isomers prefer the structure of 3a as the G–S structure, while LiB_3 prefers the structure of 3c [17].

When substituting the B atom on one of the tips of the most stable B_5, we obtain the planar lowest–energy isomer of ScB_4 (4a in Fig. 1). All MB_4 (M = Li, Al, Cr, Mn, Fe, Co,

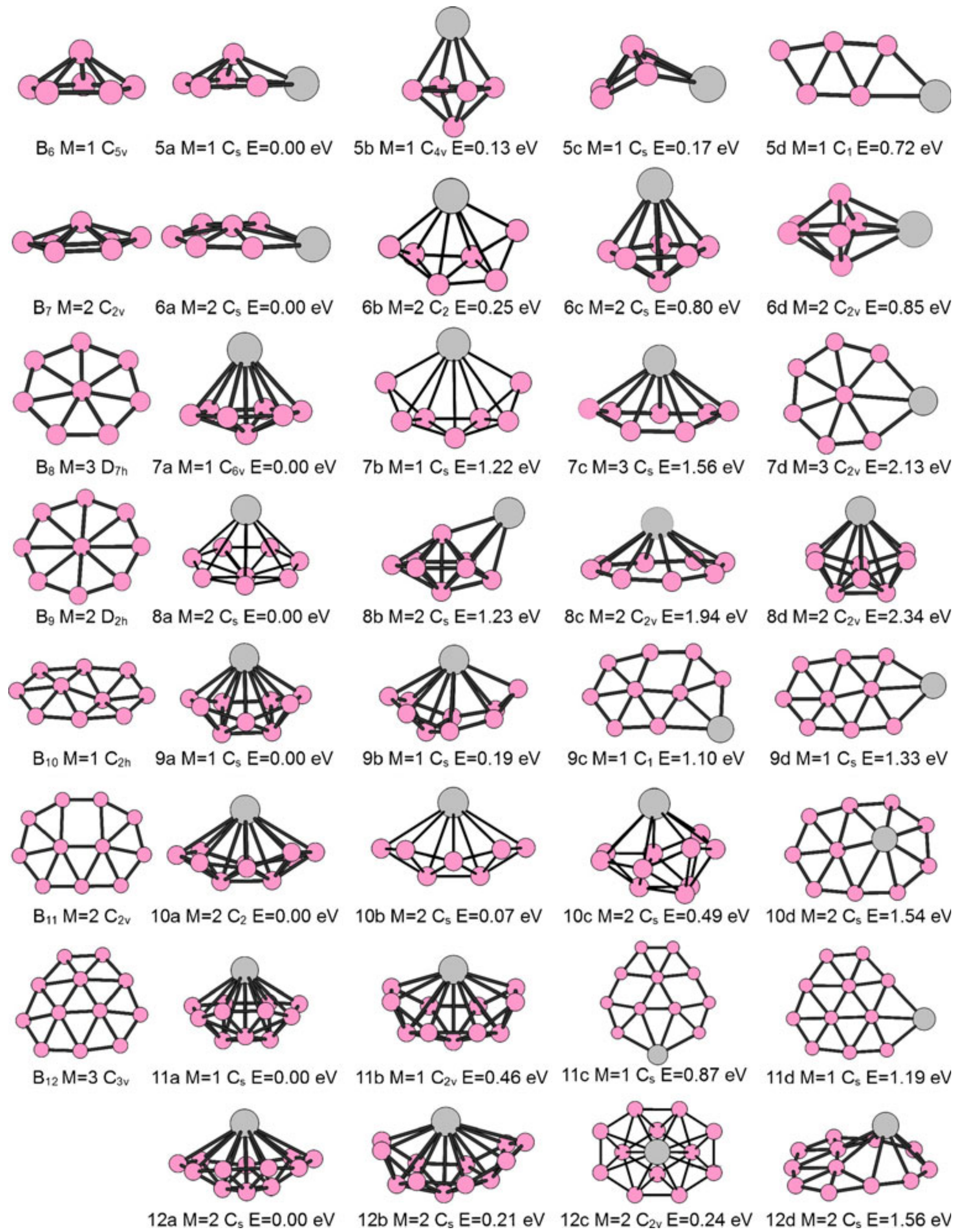

Fig. 2 Equilibrium geometries, the symmetries and spin multiplicities of the B_n (n=6–12) and ScB_n (n=5–12) structures. Relative energies (E) are given in eV

Ni) clusters prefer this pattern as G–S structure, except for TiB_4. Another ScB_4 isomer 4b, with the Sc atom capped on the bent rhombus B_4, is higher in energy than the G–S structure by 0.57 eV. The 4c is also generated by substituting a B atom of the B_5 [24, 25] by Sc atom, which is distorted to non–planar structure, being 0.62 eV higher in energy than the G–S isomer.

The most stable ScB_5 isomer (5a in Fig. 2) is originated from the most stable B_6 by replacing one circumferencial B atom by a Sc atom, being the same as the G–S structure of TiB_5 [23]. The tetragonal bipyramidal isomer 5b is 0.13 eV higher than the G–S structure in energy. Another low–lying isomer 5c in Fig. 2, which is similar to 5a in motif, with some distortions, is only 0.17 eV higher than 5a in energy. The isomer 5d is higher in energy than 5a by 0.72 eV. It should be mentioned that the G–S structures of MB_5 (M = Cr, Mn, Fe, Co, Ni) reported by Liu [15] all have planar structure.

As for the ScB_6 cluster, the G–S isomer 6a in Fig. 2 can be viewed as a circumferencial B atom of the most stable B_7 [24, 25] being substituted by a Sc atom, which is identical to that of other transition metal–doped MB_6 (M = Cr, Mn, Fe, Co, Ni) clusters [15], and different from that of AlB_6 [16, 19] and LiB_6 [17] clusters. The isomer 6b is the second low–lying isomer, in which the Sc atom is capped on a bent B_6 ribbon, being 0.25 eV higher in energy than 6a. A pentahedral dipyramidal structure 6c with Sc siting on an apex is 0.80 eV higher than 6a in energy, and another pentahedral dipyramidal structure 6d with Sc siting on the base is higher than 6a by 0.85 eV in energy.

The G–S structure of ScB_7 (7a in Fig. 2), with high C_{6v} symmetry, is formed by capping a Sc atom on the most stable B_7 isomer, being the same as other MB_7 (m = Li, Cr, Mn, Fe, Co, Ni) G–S structures. The basic framework of the B_7 cluster nearly remains intact when doped with a Sc atom. Several other isomers were considered, but they are energetically higher. For example, isomer 7b, which is formed by capping a Sc atom on a B_7 ribbon, and isomer 7c formed by capping a Sc atom on a B_7 ring, are higher in energy than 7a by 1.22 and 1.56 eV, respectively. The planer isomer 7d, originated from B_8 by substituting a circumferencial B atom by one Sc atom, is more unstable, being higher in energy than 7a by 2.13 eV.

The G–S structure of ScB_8 (8a in Fig. 2) is a heptagonal bipyramid with C_s symmetry, which was obtained by capping a Sc atom on the most stable B_8. In 8a, The B_8 distorts to a bowl–like structure. Our reported TiB_8 [23] and Böyükata reported AlB_8 [16] have the same G–S structures as ScB_8. The irregular polyhedron isomer 8b is higher by 1.23 eV in energy than the 8a. Isomer 8c, in which a Sc atom being capped on a B_8 ring, is 1.94 eV higher in energy than the 8a. A nest–like isomer 8d with a Sc atom on the surface is obtained as the low–lying isomer with further higher energy (2.34 eV) than 8a.

Both 9a and 9b in Fig. 2 have the nest–like structure. Isomer 9a, as the G–S structure of ScB_9 is more stable than 9b by 0.19 eV, which have the same structure pattern as the G–S structure of ZrB_9 [18], and slightly different from that of TiB_9. As reported, AlB_9 prefer a planer G–S structure [16, 19]. Based on the structure of B_{10}, we obtained other isomers (9c, 9d in Fig. 2) formed with the B atom at different sites of the most stable B_{10} being substituted by a Sc atom, and they are higher in energy than 9a by 1.10 and 1.33 eV, respectively.

The G–S structure of ScB_{10}, as shown in Fig. 2 as 10a, also has nest–like structure with C_2 symmetry, which is formed by capping one Sc atom on the distorted most stable B_{10}. This G–S structure is totally similar to that of ZrB_{10} and TiB_{10}. Isomer 10b has the same structure motif with 10a, but with different symmetry of C_s, which is only 0.09 eV higher in energy than 10a. Another nest–like isomer 10c is higher in energy than 10a by 0.49 eV. The quasi–planar structure 10d, which is formed by substituting a B atom of B_{11} by a Sc atom, is also obtained as low–lying isomer with further higher energy (1.54 eV).

The nest–like isomer 11a is identified as the G–S structure of ScB_{11}, which has the same structure pattern as TiB_{11} and ZrB_{11} clusters. Another nest–like structure 11b is higher in energy than 11a by 0.46 eV. Planer structures 11c and 11d, which are generated by substituting different B atoms of the most stable B_{12} by a Sc atom, are higher in energy by 0.87 eV, 1.19 eV than 11a, respectively. AlB_{11} prefer an isomer similar to 11c as its G–S structure.

Three nest–like structures were obtained as the low–lying state of ScB_{12} (12a, 12b and 12c in Fig. 2). Isomers 12b and 12c only are higher in energy than the G–S structure 12a by 0.21 and 0.24 eV, respectively. The G–S structure of ScB_{12} is the same as that of TiB_{12} and ZrB_{12}, which formed by capping one Sc atom on the most stable B_{12} cluster. Isomer 12d, which originated from the most stable B_{13} with one central B atom substituted by a Sc atom, is higher in energy than 12a by 1.56 eV.

From above discussion, it can be found that the G–S isomers of ScB_n have planar or quasi–planar structure when $n \leq 6$. All these G–S isomers can be viewed as a B atom of the corresponding B_{n+1} cluster being substituted by a Sc atom. From $n \geq 7$, the G–S isomers favor nest–like structure, in which the Sc atom sits on a nest–like B_n cluster. In all the ScB_n G–S isomers, except for ScB_6, ScB_9 and ScB_{11}, the B_n moieties nearly remain the geometric pattern of the G–S isomer of B_n, with some out–plane distortions in ScB_8, ScB_{10} and ScB_{12}. In all the G–S isomers of ScB_n, the Sc atom favors to locate either at the outer side or above the surface of the B_n clusters, not the center of the clusters. The site of Sc atom in the ScB_n is favored for the gas adsorption on the cluster.

Relative stability

In cluster science, the second–order difference of cluster energies is a sensitive quantity to reflect the relative stabilities of the clusters [15–19, 26]. The second–order difference of cluster energies can be defined by the following reaction and formula:

$$2ScB_n \rightarrow ScB_{n+1} + ScB_{n-1}, \Delta^2E(n) = E(n+1) + E(n-1) - 2E(n), \quad (1)$$

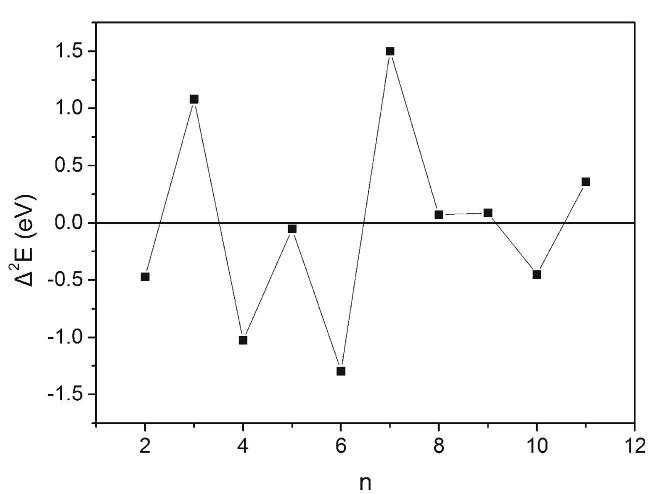

Fig. 3 The second–order differences of ScB_n clusters energies (Δ^2E/eV)

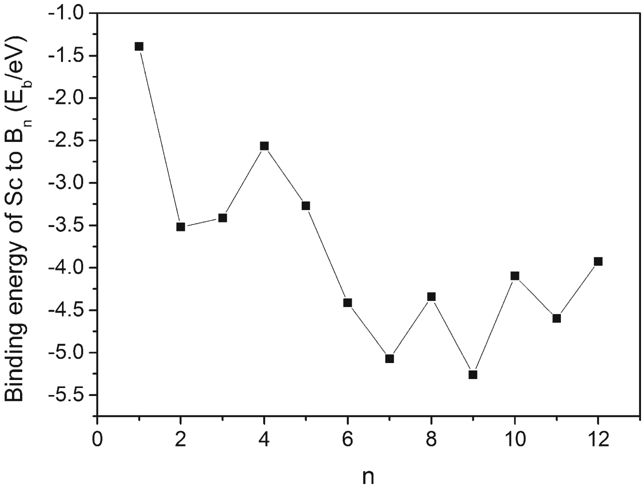

Fig. 4 The binding energies (E_b/eV) of Sc to B_n clusters

where E(n) is the total energy of the ScB_n G–S isomer. As shown in Fig. 3, ScB_n with n=3, 7, 8, 9 and 11 have positive Δ^2E, which indicates that these clusters possess higher stability. It is worth pointing out that for TiB_n (n=1–12), TiB_n (n=3, 7, 8) also were identified as magic stable clusters. The theoretical calculations also showed that the MB_7 (M = Cr, Fe, Co, Ni and Zr) clusters have outstanding stability. The stabilities of MB_7 might be caused by both geometric effect and electronic effect. The stable B_7 cluster has a bowl like structure, which nearly remains intact in MB_7. The outstanding stabilities of MB_7 promise them as basic blocks to build hydrogen storage materials.

As promising candidate materials for hydrogen storage, the clustering of metal atoms on the doped B_n nanostructures not only significantly changes the nature of hydrogen bonding but also greatly reduces the weight percentage of hydrogen storage [27]. It is expected that the large binding energy (E_b) between metal and boron cluster will restrain the

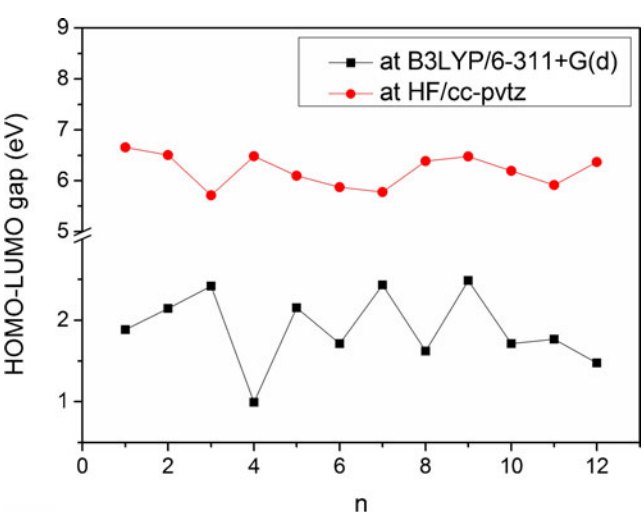

Fig. 5 The HOMO–LUMO gaps of ScB_n clusters in eV

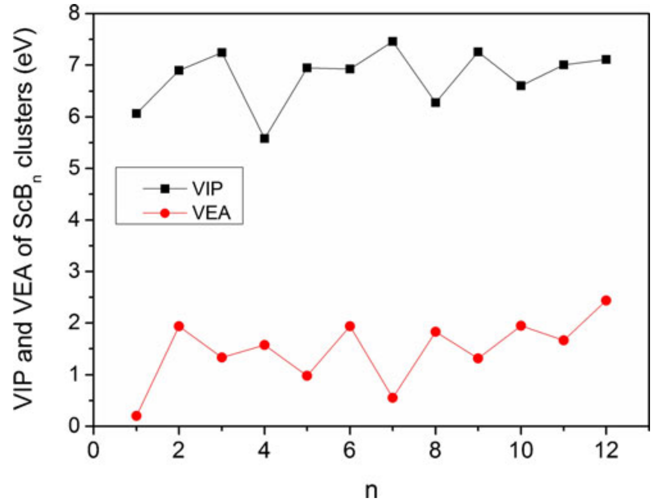

Fig. 6 The vertical ionization potentials (VIP) and vertical electron affinities (VEA) of ScB_n clusters in eV

clustering of metal atoms. The E_b is also an important index to estimate the stability of ScB_n clusters. The E_b of Sc to B_n can be defined by the following reaction and formula:

$$B_n + Sc = ScB_n, E_b = E(ScB_n) - E(B_n) - E(Sc), \qquad (2)$$

where $E(ScB_n)$, $E(B_n)$ and E(Sc) are the total energies of optimized ScB_n, B_n clusters and Sc atom. The initio structures of B_n were taken from ref. [22]. As shown in Fig. 4, when $n \geq 6$, the binding energies (E_b) of Sc to all B_n are more negative than the cohesive energy of Sc bulk (–3.9 eV), and also more negtive than the average binding energy of Sc atom in Sc_n clusters [28]. When $n \geq 6$, the change of E_b

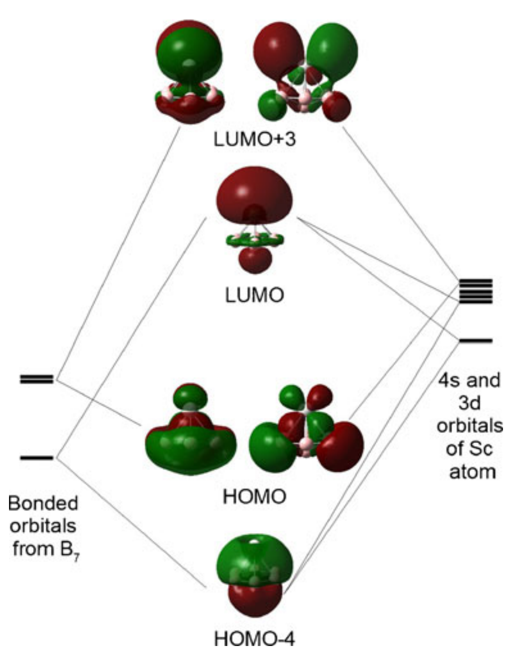

Fig. 7 The molecular orbitals reflecting the binding between Sc atom and B_7 unit in ScB_7 cluster

becomes more regular. Namely, the ScB_n clusters with odd n have more negative E_b than those with even n. So, from the viewpoint of E_b, the ScB_n with $n=7$, 9 and 11 are more stable than that with $n=8$, 10 and 12, which is consistent with the result of Δ^2E analysis, except for ScB_8.

A useful index of examining the kinetic stability and the chemical reactivity of the clusters is the HOMO–LUMO energy gap [16, 18, 29]. However, the calculated energy gap is very sensitive to the calculation method. The size dependence of the HOMO–LUMO gaps calculated both at B3LYP/6– 311+G(d) and HF/cc–pvtz (from the CCSD (T)/cc-pvtz calculations) are shown in Fig. 5. It is clear that the HOMO–LUMO gaps calculated by Hartree–Fock method are larger than that by B3LYP method. Moreover, they have differrent relative values. For example, the gap of ScB_7 is larger than that of ScB_8 under B3LYP calculations, with the opposite being the case under HF calculations. Under B3LYP calculations, the change of HOMO–LUMO gaps has an obvious trend. All the ScB_n with close–shelled electronic structure have larger HOMO–LUMO gaps than their neighbors, especially the remarkable local peaks being found for $n=3$, 7 and 9. The large HOMO–LUMO gaps of these isomers imply that these clusters have more strong chemical stabilities than their neighbors.

Moreover, to analyze the size–dependent electronic stability of the G–S isomers of ScB_n clusters, we have calculated the vertical ionization potential ($VIP = E[ScB_n^+] - E[ScB_n]$) and vertical electron affinity ($VEA = E[ScB_n] - E[ScB_n^-]$) of every ScB_n G–S isomer to estimate the required energy to remove or add one electron on it without any structural relaxation. As shown in Fig. 6, the first and second highest values of VIP are obtained for ScB_7 and ScB_9, respectively, which indicates these two isomers are more stable against being ionized. The trend of VEA is more regular than that of VIP, which exhibits an odd–even oscillational character. Namely, ScB_n clusters with even electronic number have smaller VEA than those with odd electronic number. The low VEA should be related with their stabilities. The lowest VEA of ScB cluster is mainly caused by its special electronic structure. It is interesting that ScB_7 also has a small VEA, which indicates its stability against obtaining one electron.

Up to now, among all the studied clusters, ScB_7 is found as the magic–number cluster, which has pronounced peaks for the second–order difference of energies (Δ^2E), the binding energy (E_b), the HOMO–LUMO gap, the VIP and VEA. As we mentioned above, the stability of ScB_7 might be related to both its geometric and electronic structure. So, it is interesting to have an analysis about its molecular orbitals. Figure 7 lists the orbitals contributing to the binding between Sc atom and B_7 cluster. The HOMO orbital of ScB_7 is a pair of degenerated orbitals, which clearly consists of the d orbitals of Sc and a pair of degenerated bonded orbitals of B_7 cluster. Their corresponding anti–bonded orbital is also shown in Fig. 7, denoted as LUMO+3, which also is a pair of degenerated orbitals. The LUMO of ScB_7 is clearly an anti–bonded orbital, which is comprised by the *d–s* hybridized orbital of Sc atom (with more *s* component) and a bonded orbital of B_7 cluster. The corresponding bonded orbital of the LUMO is shown in Fig. 7 as HOMO–4. So, the HOMO–4 and HOMO contribute to the stability of ScB_7. The anti–bonded character of the LUMO and bonded character of HOMO of ScB_7 result in its larger HOMO–LUMO gap, larger VIP and smaller VEA, namely, good electronic stability.

Conclusions

A systematical CCSD(T)/cc–pvtz investigation on the growth pattern, stability and electronic properties of the ScB_n clusters has been carried out with extensive calculations at $n=1$–12. The ScB_n G–S isomers favor planar or quasi–planar structure when $n\leq6$, and from $n=7$ they have nest–like structure. In the G–S isomers of ScB_n, the B_n moieties nearly maintain the pattern of the G–S isomer of B_n cluster except for ScB_6, ScB_9 and ScB_{11}. However out–plane distortion of B_n moiety occurs in ScB_5, ScB_8, ScB_{10} and ScB_{12}. The calculated second–order differences of energies show that the ScB_3, ScB_7, ScB_8, ScB_9 and ScB_{11} clusters possess relatively higher stability. The ScB_7 cluster with C_{6v} symmetry represents the most stable structure, as indicated by the calculated second–order difference of energies (Δ^2E), binding energy (E_b), HOMO–LUMO gap, vertical ionization potential (VIP) and vertical electron affinity (VEA). So, we think that ScB_7 may be a promising nano–block to fabric the hydrogen storage materials, given the kubas [30] interaction between transition metal atom and hydrogen molecules.

Acknowledgments This work was supported by National Basic Research (973) Program of China (No. 210CB635110) and National Natural Science Foundation of China (21031003 and 21103101).

References

1. Meng S, Kaxiras E, Zhang Z (2007) Nano Lett 7:663
2. Li F, Zhao J, Chen Z (2010) Nanotechnology 21:134006
3. Zhao Y, Kim Y-H, Dillon AC, Heben MJ, Zhang SB (2005) Phys Rev Lett 94:155504
4. Yildirim T, Íñiguez J, Ciraci S (2005) Phys Rev B 72:153403
5. Wu G, Wang JL, Zhang X, Zhu L (2009) J Phys Chem C 113:7052
6. Zhao YF, Lusk MT, Dillon AC, Heben MJ, Zhang SB (2008) Nano Lett 8:157
7. Li Y, Zhou G, Li J, Gu B-L, Duan W (2008) J Phys Chem C 112:19268

8. Zhao J, Wang L, Li F, Chen Z (2010) J Phys Chem A 114:9969
9. Quarles KD, Kah CB, Gunasinghe RN, Musin RN, Wang X (2011) J Chem Theory Comput 7:2017
10. Zhai HJ, Wang LS, Zubare DY, Boldyre AI (2006) J Phys Chem A 110:1689
11. Alexandrova AN, Boldyrev AI, Zhai HJ, Wang LS (2005) J Chem Phys 122:054313
12. Alexandrova AN, Zhai HJ, Wang LS, Boldyrev AI (2004) Inorg Chem 43:3552
13. Lei XL, Zhu HJ, Ge GX, Wang XM, Luo YM (2008) Acta Phys Sin 57:5491
14. Yang Z, Yan YL, Zhao WJ, Lei XL, Ge GX, Luo YH (2007) Acta Phys Sin 56:2590
15. Liu X, Zhao GF, Guo LJ, Jing Q, Luo YH (2007) Phys Rev A 75:063201
16. Böyükata M, Güvenc ZB (2011) J Alloys Compd 509:4214
17. Truong BT, Nguyen MT (2010) Chem Phys 375:35
18. Yao J-G, Wang X-W, Wang Y-X (2008) Chem Phys 351:1
19. Feng XJ, Luo YH (2007) J Phys Chem A 111:2420
20. Becke AD (1993) J Chem Phys 98:5648
21. Lee C, Yang W, Parr RG (1988) Phys Rev B 37:785
22. Frisch MJ, Trucks GW, Schlegel HB, Scuseria GE, Robb MA, Cheeseman JR, Montgomery JA Jr, Vreven T, Kudin KN, Burant JC, Millam JM, Iyengar SS, Tomasi J, Barone V, Mennucci B, Cossi M, Scalmani G, Rega N, Petersson GA, Nakatsuji H, Hada M, Ehara M, Toyota K, Fukuda R, Hasegawa J, Ishida M, Nakajima T, Honda Y, Kitao O, Nakai H, Klene M, Li X, Knox JE, Hratchian HP, Cross JB, Bakken V, Adamo C, Jaramillo J, Gomperts R, Stratmann RE, Yazyev O, Austin AJ, Cammi R, Pomelli C, Ochterski JW, Ayala PY, Morokuma K, Voth GA, Salvador P, Dannenberg JJ, Zakrzewski VG, Dapprich S, Daniels AD, Strain MC, Farkas O, Malick DK, Rabuck AD, Raghavachari K, Foresman JB, Ortiz JV, Cui Q, Baboul AG, Clifford S, Cioslowski J, Stefanov BB, Liu G, Liashenko A, Piskorz P, Komaromi I, Martin RL, Fox DJ, Keith T, Al-Laham MA, Peng CY, Nanayakkara A, Challacombe M, Gill PMW, Johnson B, Chen W, Wong MW, Gonzalez C, Pople JA (2004) Gaussian 03, Revision C. 01. Gaussian, Inc, Wallingford
23. Wang J-F, Jia J, Ma L-J, Wu H-S (2012) Acta Chim Sin 70:1643
24. Alexandrova AN, Boldyrev AI, Zhai HJ, Wang LS (2006) Coord Chem Rev 250:2811
25. Boustani I (1997) Phys Rev B 55:16426
26. Wang JL, Wang GH, Zhao JJ (2001) Phys Rev B 64:205411
27. Sun Q, Wang Q, Jena P, Kawazoe K (2005) J Am Chem Soc 127:14583
28. Wang J (2007) Phys Rev B 75:155422
29. Pearson RG (1993) Acc Chem Res 26:250
30. Kubas GJ (2001) J Organomet Chem 635:37